ESA Discovery and Preparation – OSIP

Campaign on Remote Sensing of Plastic Marine Litter

Characterization of light polarization properties of virgin and marine-harvested plastic litter toward remote-sensing mapping of ocean plastics

Ocean Plastics Polarization Properties (OP^3)

Executive Summary

Issue 1.0

Date: 16 December 2022

Ref.: ESA_OP3_ES_Dec22

ESA contract no. 4000132037/20/NL/GLC

Project name: **Ocean Plastics Polarization Properties (OP3)**

Document title: **Final Report**

Reference no.: **ESA_OP3_FR_Dec22**

Issue date: **16-12-2022**

Issue and revision: **1.0**

ESA contract no.: **4000132037/20/NL/GLC**

Organization: **Carl von Ossietzky Universität Oldenburg, Oldenburg, Germany**

Leiden University, The Netherlands

TH-Consulting, Nice, France

	Name	Company or Institute	Signature
Prepared by	Tristan Harmel	TH-Consulting	
	Shungu Garaba	Carl von Ossietzky Universität	
	Olivier Burggraaff	Leiden University	
Reviewed by			
Distribution list	Paolo Corradi Leopold Summerer	ESA/ESTEC ESA/ESTEC	

Table of Contents

1. Scope of document

The scope of this executive summary is to highlight the scientific experimental and evidence-based research that was conducted in the OP3 project. The OP3 project was funded from 2020 – 2022 by the Discovery Element of the European Space Agency's Basic Activities, in the frame of the Discovery Campaign on Remote Sensing for Plastic Marine Litter. The primary team of OP3 was from Germany (Carl von Ossietzky Universität Oldenburg), France (TH Consulting), The Netherlands (Leiden University) and collaborations were realised through experiments-of-opportunity with scientists at various institutes (e.g., Deltares, Netherlands). This executive summary provides the key advances relevant to potential use of polarimetric information derived from remote sensing technologies and full radiative transfer computations to monitor aquatic plastic litter.

2. Overview

2.1 Motivation

Monitoring strategies for aquatic plastic litter using remote sensing is foreseen to complement and support future continuous observations of pollution at wide covering geo-spatial scales. The remote sensing technologies and algorithms are thus expected to be robust/sustainable. In terms of the algorithms there is a requirement that the algorithms are also based on fundamental and well characterized features (e.g., from optical, radar, laser, microwave sensors). Among the important optical characteristics is the polarization of light by plastics which we presume could be useful to better understand remote sensing information in addition to reflectance shape and magnitude. Spectropolarimetry is expected to contribute towards approaches that mitigate uncertainties resulting from sea surface reflected glint and atmospheric correction e.g., (Gilerson et al., 2020; Harmel and Chami, 2013).

2.2 Plan of action

Polarimetric properties of virgin and weathered plastic litter are not well documented in open-access (Garaba and Harmel, 2022), therefore OP3 was proposed to conduct relevant groundwork. The research aimed at developing algorithms for data handling, processing and documenting polarization characteristics of the tested plastics. In addition, a theoretical study was conducted to propagate the plastic optical signature within the atmosphere-water system with a specific focus on intensity and polarization of light at the top-of-atmosphere.

Three sensors were assessed as part of the plan to establish a reference library of polarimetric properties of virgin and weathered plastics. A SPECIM-IQ hyperspectral camera (VNIR, 400 - 1000 nm) and a compact multispectral FLIR BlackFly S USB3 polarimetric Red-Green-Blue (RGB) sensor were used to capture images of target samples. Point measurements (~400 - 900 nm) were also collected using the unique hyperspectral spectropolarimeter GroundSPEX (van Harten et al., 2014). Open-source Python-based packages were developed to process the imagery captured in the project. The developed open-source packages are presumed simple to use, easy to adapt and powerful tools for scientific application. The initial purpose of the packages is analyses of acquired relevant images and generating quality-controlled datasets of plastic litter polarization properties that can also be easily adapted for similar research. The full radiative transfer simulations were important in exploring the (i) top-of-atmosphere signature of floating and submerged macroplastics, (ii) in-water, above-water and TOA polarization signature (Stokes vector) of nano and micro-plastic particles in suspension.

2.3 Objectives

The objectives of this project were to generate and produce:

[O-1] Protocols for polarimetric data collection and processing for above-water observations relevant to plastic litter monitoring.

[O-2] Reference dataset for polarization spectra of plastic litter of various sizes and shapes.

[O-3] Develop and evaluate satellite retrieval (plastic litter) algorithms for prospective application to the historic and next-generation polarimetric missions.

3. Project milestones

3.1 Linearity test of FLIR polarimetric imager

The linearity of the FLIR camera, that is checking whether 2x the radiance gives 2x the digital number, was characterized. The camera, without any lens attached, was illuminated with an LDLS ISTEQ XWS-30 light source and images were taken at varying exposure times (Burggraaff et al., 2019). A set of 250 images each obtained at 43 different exposure times showed that our FLIR camera response had a very strong linearity with Pearson *r > 0.9997* in every pixel (Figure 1). Further work is required to fully characterize the response curve at its extreme ends (black level and saturation limit), as well as other aspects of the camera including gain, polarization efficiency, and spectral response.

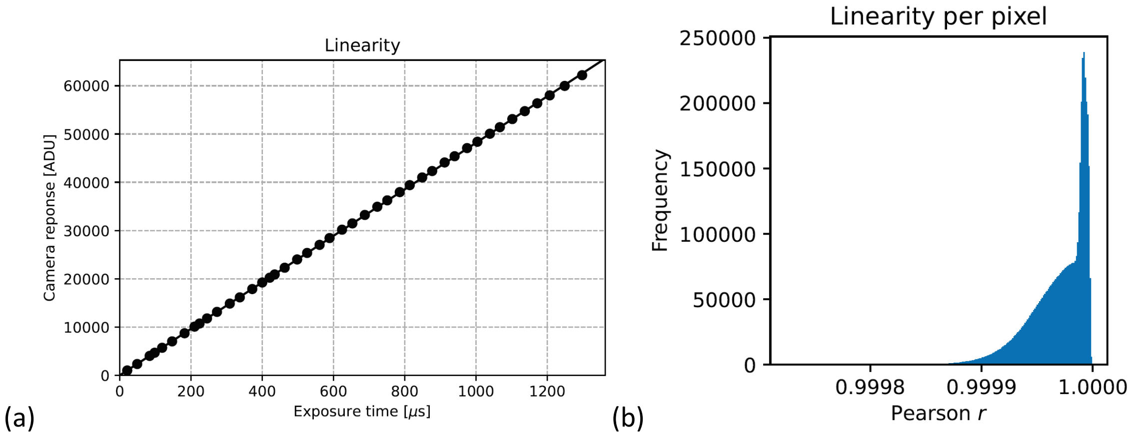

Figure 1. (a) Example response of a randomly chosen pixel on the FLIR sensor with increasing exposure time. Each point corresponds to the average of 250 images and a best linear fit. (b) Histogram of the linearity of all pixels on the FLIR sensor expressed in Pearson r correlation coefficient and lowest value was r = 0.9997.

3.2 Laboratory and tank experiments

Laboratory based images were collected using the SPECIM-IQ camera equipped with linear polarizer (~400 – 800 nm) to assess the polarization signature of plastic targets. The first goal was to derive the reflectance measurements with and without polarizer to quantify the polarizing characteristics of common plastic objects susceptible to be encountered in polluted marine environment. An open-source package was developed to process and visualize the captured hyperspectral images. The observed hyperspectral images were processed to get them in reflectance unit for the two modalities of acquisition i.e., with or without mounted polarizer (**Figure 2**).

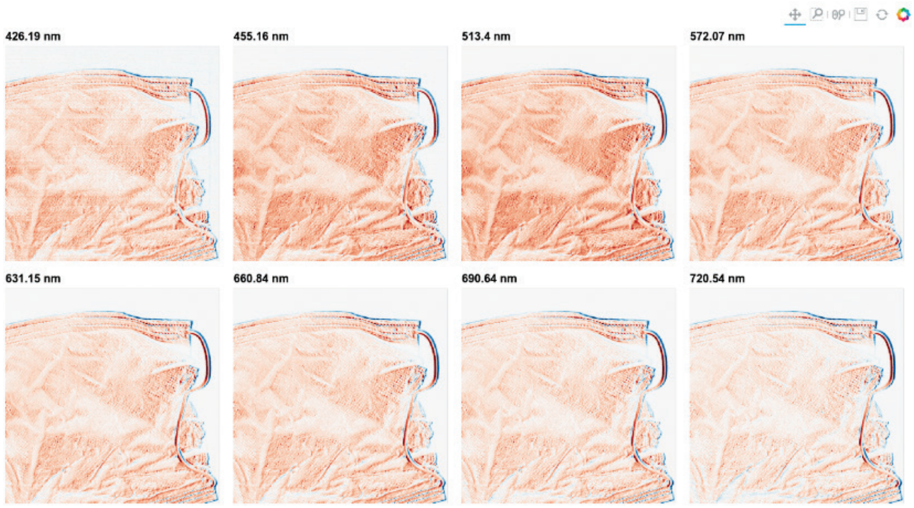

Figure 2. Difference between total and polarized reflectance for some selected wavelength band of the SPECIM-IQ device.

The package was built with a tool to manually select a region of interest as a rectangle within the image that automatically extracts the respective reflectance spectra. Examples showing the polarization data processing in Python using *Jupyter Notebook* along the acquired image (**Figure 3**).

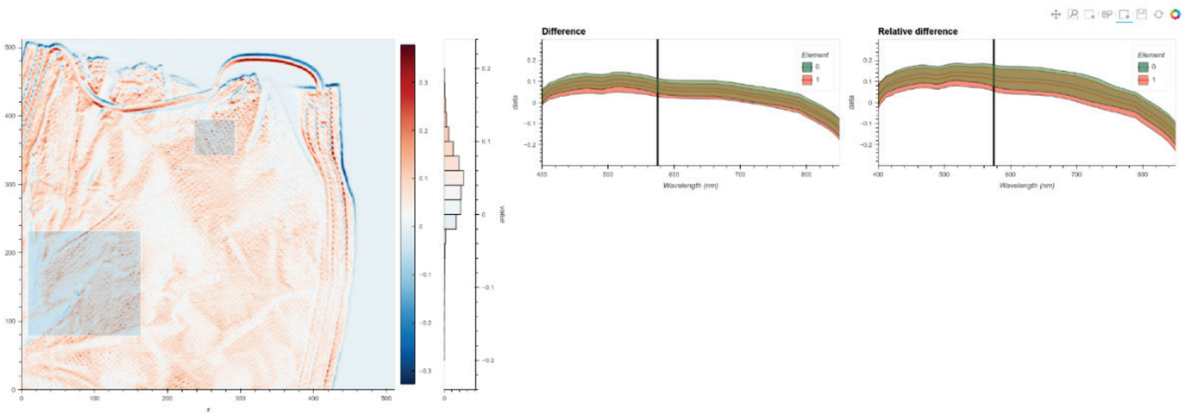

Figure 3. Example of interactive spectra extraction: (left) image in false colour where polygons are manually drawn, (right) average spectra and standard deviation envelope of spectra extracted from the selected polygon.

3.3 Lake Berre field campaign

The FLIR BlackFly S USB3 camera was used during an experiment of opportunity in October 2021 on Lake Berre in France (**Figure 4**). Raw images were processed using an open-source Python library (https://github.com/elerac/polanalyser). Images were demosaiced to obtain pixels provided by the four polarizer orientations (0°, 45°, 90°, 135°) and the three RGB spectral wavebands producing twelve distinct images.

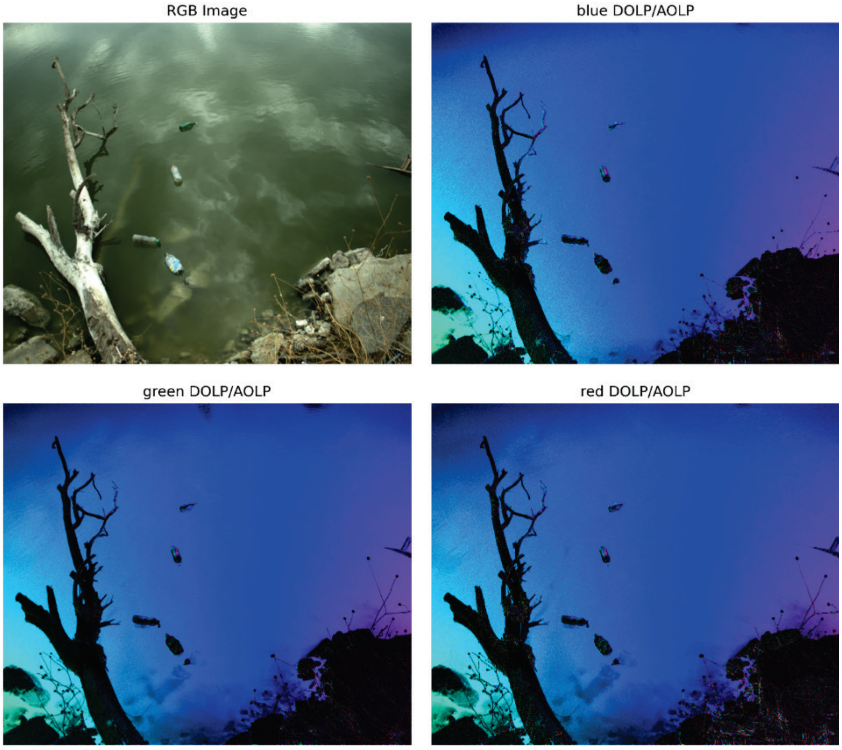

Figure 4. FLIR BlackFly S USB3 camera images of a scene with wood and floating plastics plastic-free water surface under clear sky. Top-left corner RGB image, the other images correspond to Degree of Linear Polarization, DOLP (brightness) and Angle of Linear Polarization, AOLP (colours) for the three RGB channels of the camera.

3.4 Experiment campaign at Deltares

A first session of tests for microwave and optical sensors was conducted at the Atlantic Basin at Deltares in The Netherlands, on 14 October 2021, in the frame of a multi-team campaign partially funded by ESA. The Deltares Atlantic Basin is a flume of 8.7 m wide and 75 m long, wherein both waves and currents can be generated. The FLIR BlackFly S USB3 camera captured images containing a variety of wave and lighting conditions (**Figure 5**).

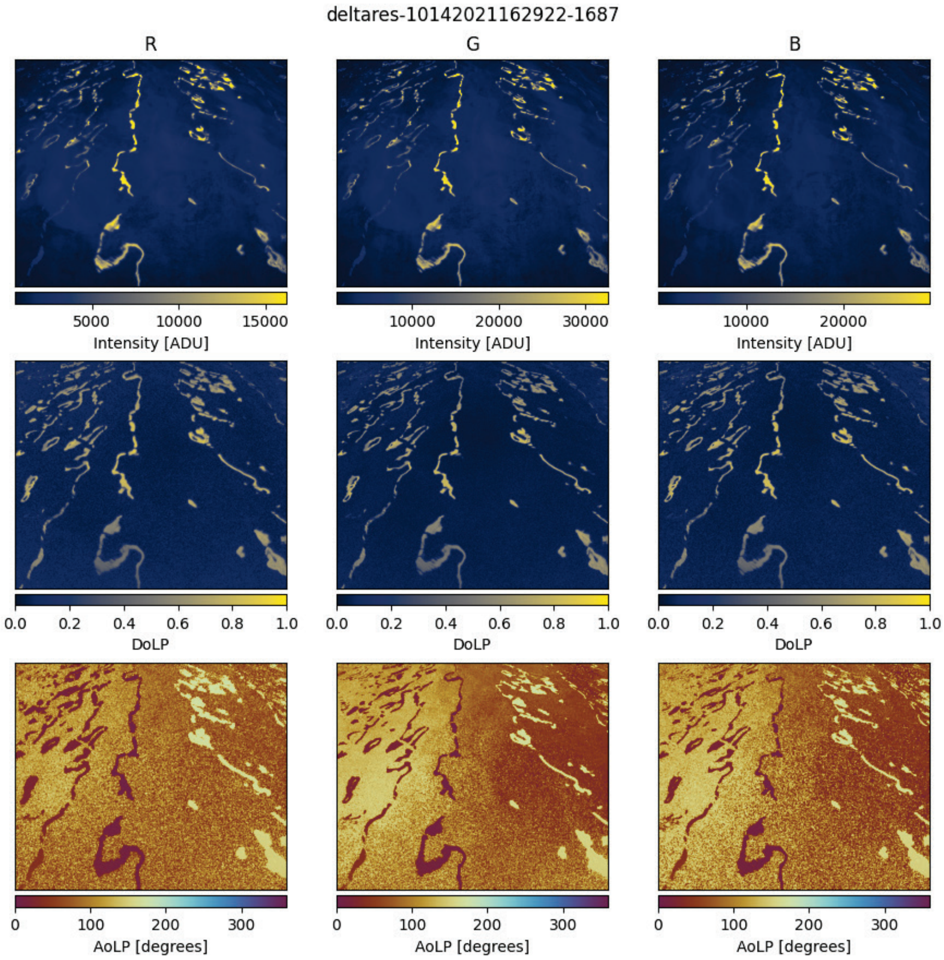

Figure 5. Teledyne FLIR BlackFly S USB3 BFS-U3-51S5PC-C camera observations of wave motion in the Deltares Atlantic Basin in polarized light. The three columns correspond to the red, green, and blue (RGB) spectral filters of the camera. The rows show the observed intensity or radiance in analogue-digital units (ADU), i.e. camera counts, and the degree and angle of linear polarisation (DoLP and AoLP, respectively). The direct reflection of light from the ceiling fluorescent lights is clearly visible as columns of bright, highly polarised light, distorted by the wave fronts.

The images were captured under ambient fluorescent lighting at the ceiling of the facility or an LED lamp. All experiments with the LED lamp also had the ceiling fluorescent lights. It is assumed the non-optimal light conditions limit the information that can be derived from the images suggesting qualitative analyses are feasible and less quantitative. During the campaign it was observed that the light sources were very heterogeneous having a less well-defined illumination with very narrow spectral lines.

Further detailed experiments were conducted at the indoor Deltares Atlantic basin from 24 to 28 January 2022. Polarimetric measurements of various plastic samples under a set of simulated wave conditions were acquired. The FLIR camera was mounted underneath a moveable metal bridge across the basin looking upstream (**Figure 6**).

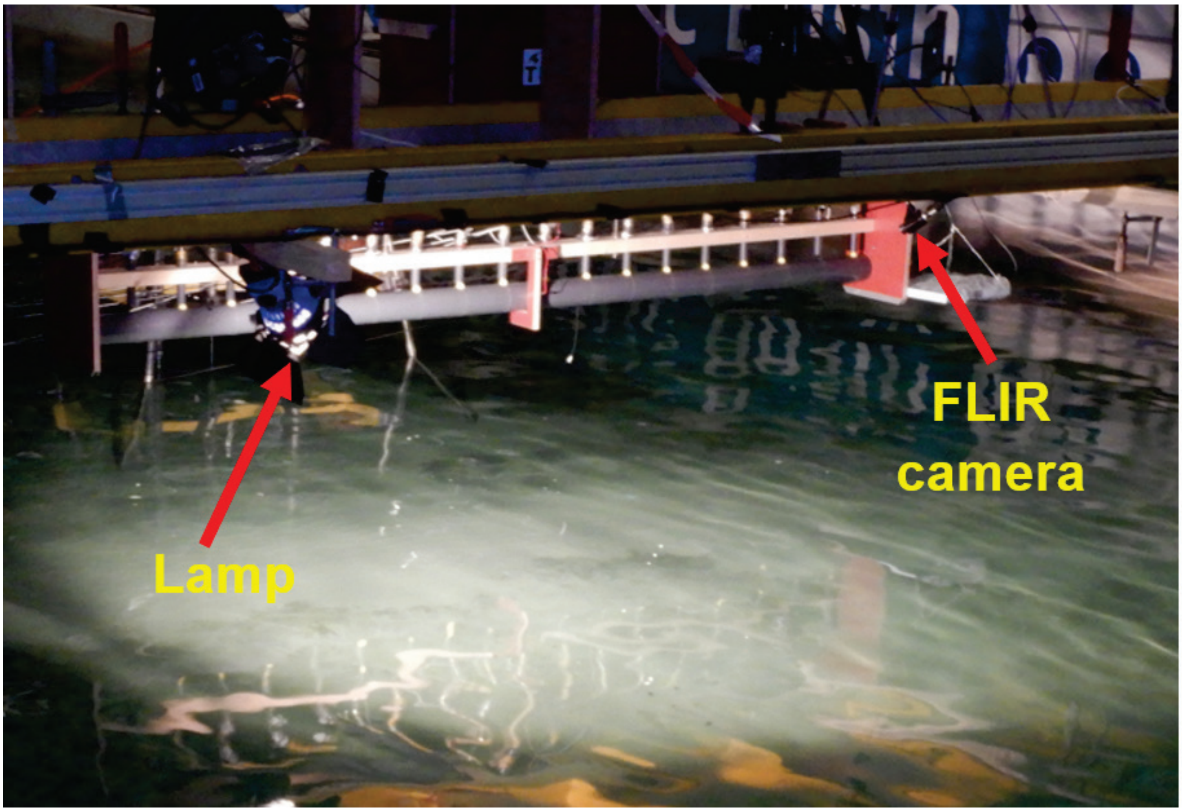

Figure 6. Position and alignment of the ARRILITE 750 Plus with a 575 W HPL halogen tungsten lamp (red circle) and Teledyne FLIR BlackFly S USB3 BFS-U3-51S5PC-C camera (yellow circle) under the bridge from 24 to 28 January 2022 during the Deltares campaign**.**

Lighting was from a halogen tungsten lamp whilst the bridge provided some shading from the fluorescent ceiling lights. The camera and lamp were both pointed at the water at ~40° from nadir at an azimuthal angle of ~135° between light source and FLIR BlackFly S USB3 camera. The camera and lamp were moved and realigned several times and it was concluded that due to the data being relatively heterogeneous gathered observations were appropriate for qualitative and less quantitative analyses. Multiple adjustments were done throughout the week to mitigate surface reflected glint from the fluorescent ceiling lights as well as other structure to optimize the field-of-view of the camera. Further measurements between 31 January and 04 February 2022 the FLIR camera was mounted on top of GroundSPEX after removal from under the bridge (**Figure 6**). For the whole campaign, GroundSPEX was positioned at the far end of the basin, looking diagonally upstream. The region of interest was determined by pointing a laser beam then directing the additional halogen tungsten lamp in the same area. Additionally, the lamp was manually aligned by observing the highest signal detected by GroundSPEX. GroundSPEX was pointed towards using an integrated pan-tilt sensor. Spectra was gathered with GroundSPEX (4,3 GB) and imaged from the FLIR camera (1,9 TB). Many of these observations were captured simultaneously using the whole suite of sensors for planned inter-comparison analyses.

3.5 Theoretical modelling

In parallel to the laboratory and fieldwork experiments, we performed theoretical investigation on micro and macro plastics through optical and radiative transfer modelling to assess the potential polarization signature of different plastic compounds. We constructed a comprehensive set of computations with the coupling of Mie-theory simulations with full vector radiative transfer computations. Those computations were conducted based on the different refractive index values and for variable size distributions (from submicron to millimetre sizes). First, the scattering matrices potentially attached to actual in-water nano- or micro-plastics were computed and saved into look-up table files (**Figure 7**).

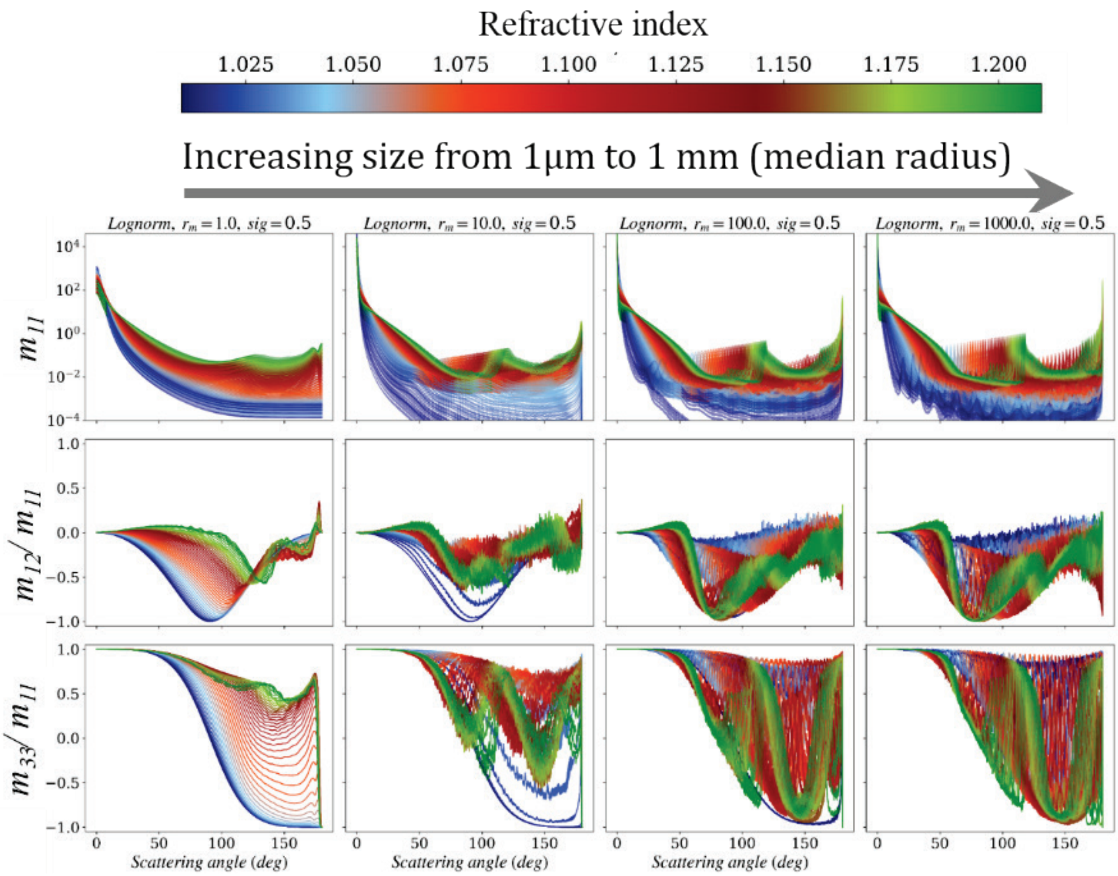

Figure 7. Scattering matrix terms obtained for a comprehensive set of microphysical parameters (e.g., size distribution, refractive index).

Based on these first findings, we assessed the directional signal in intensity and polarization at the in-water, above-water and top-of-atmosphere levels (**Figure 8**).

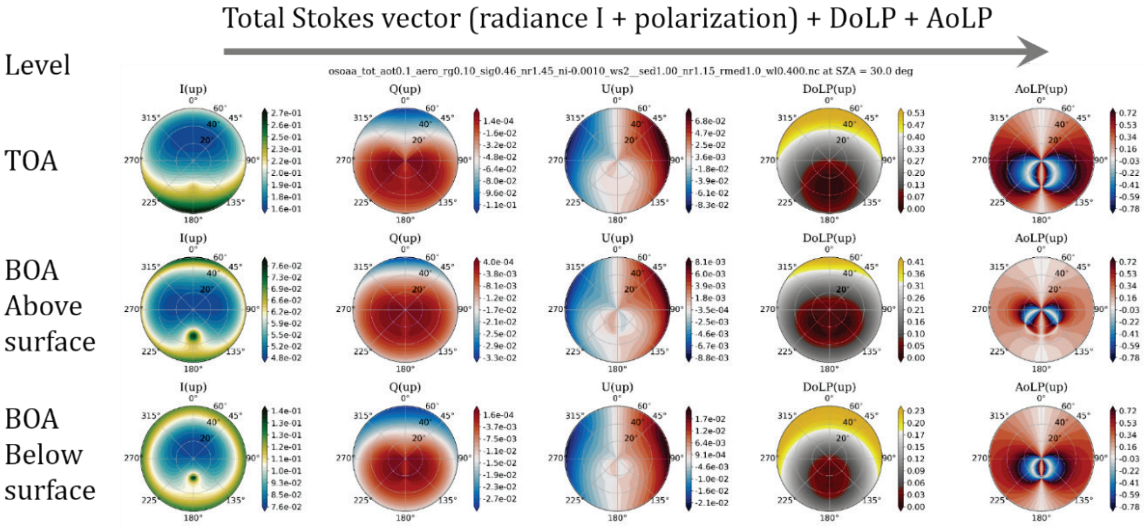

Figure 8. Stokes vector parameters (I, Q and U) at 400 nm as well as the degree and angle of linear polarization at three different levels in the atmosphere-water system: TOA for top-of-atmosphere, BOA for bottom-of-atmosphere just above and just beneath the air-water interface. In this example, the plastic grain size distribution is log-normal with a median radius of 1 µm. The sun zenith angle was set to 30°.

As seen from (**Figure 9**), the directional optical signal is sensitive to the concentration in plastic of micrometre size both in intensity (I term) and in polarization (see degree and angle of linear polarization).

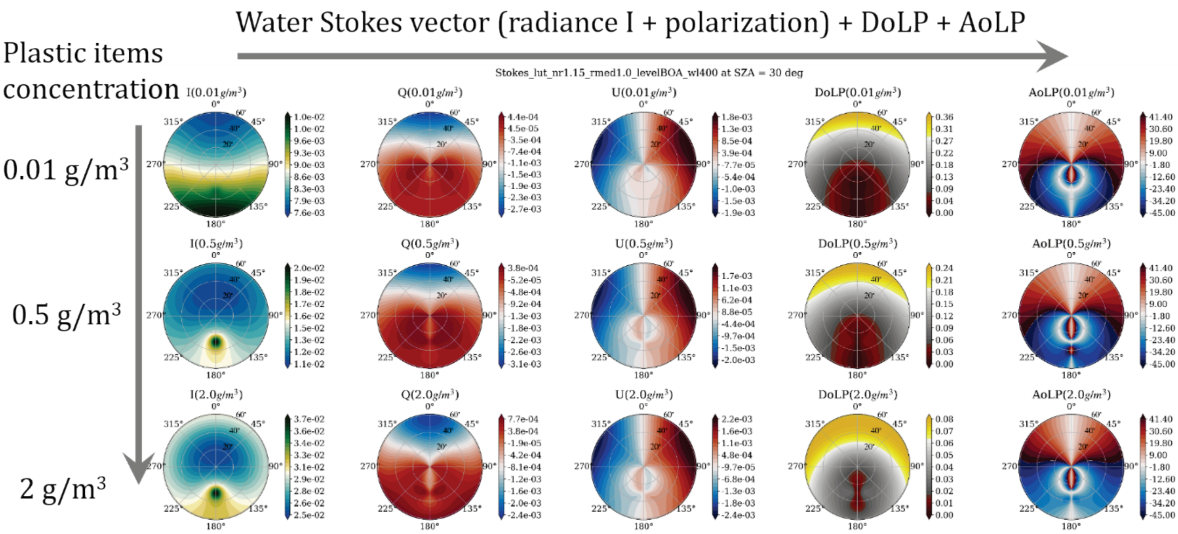

Figure 9. Stokes vector parameters (I, Q and U) at 400 nm as well as the degree and angle of linear polarization as seen just above the water surface for three different concentrations (rows) of plastic-like suspension. In this example, the plastic grain size distribution is log-normal with a mean radius of 1 µm. The sun zenith angle was set to 30°.

From those directional simulations, spectral parameters can be extracted from different viewing geometry configurations (**Figure 10**).

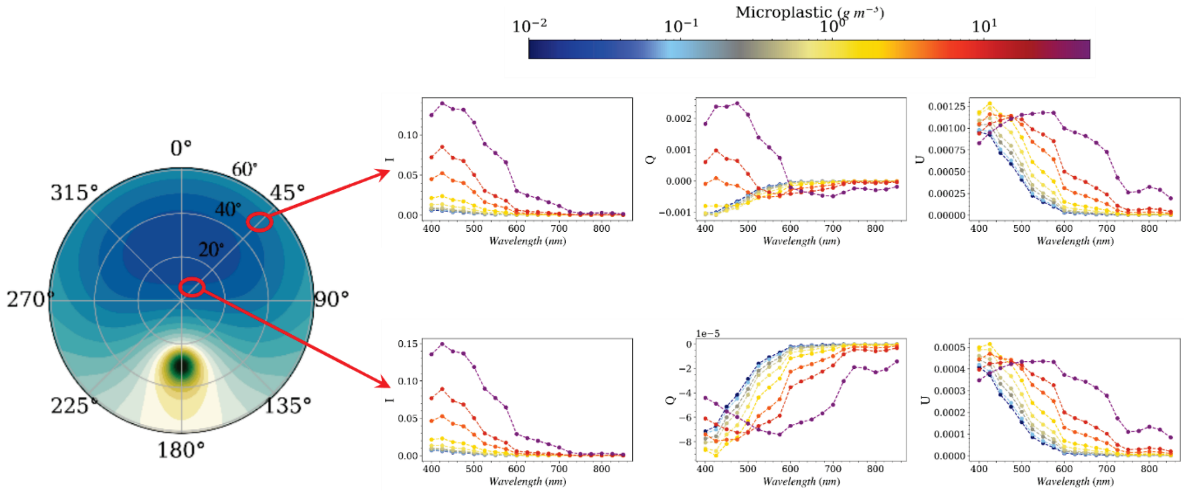

Figure 10. Examples of the spectral Stokes parameters (I, Q and U) just above water surface extracted for two combinations of solar, viewing and azimuth angles, and several concentrations of microplastics.

Figure 11 and **Figure 12** show such results for typical geometries of observation and a wide range of microplastic concentrations for micrometre and millimetre size distributions, respectively. Future works are planned first to exploit those results from in situ spectro-polarimetric data that will be collected by the Expedition 7th continent, and second, to incorporate more complex particle shapes and structures within the single scattering modelling encompassing the effects of bio-fouling of the suspended material.

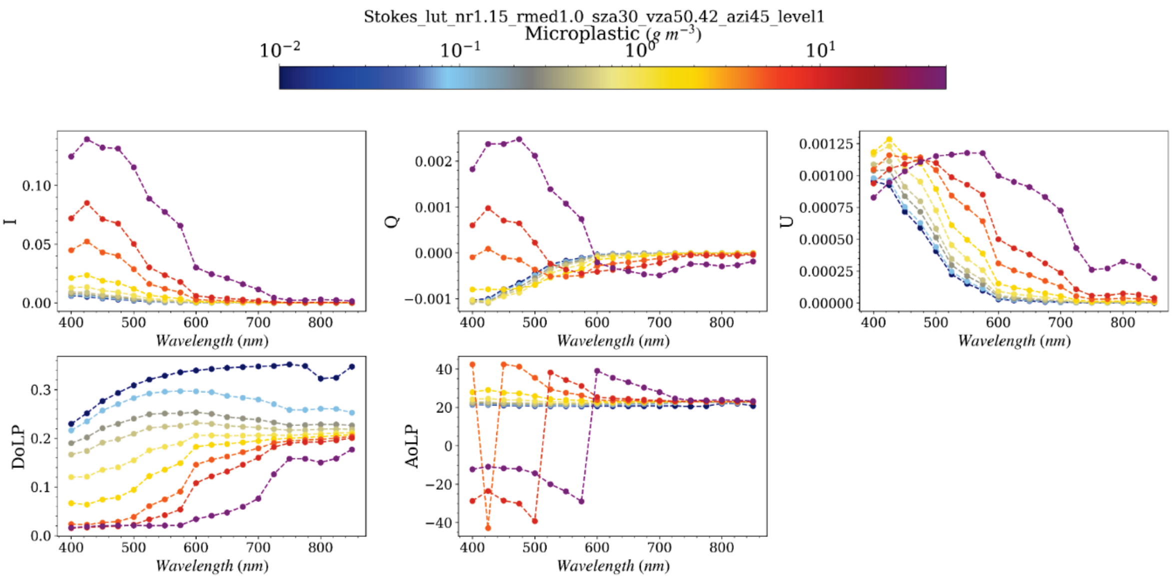

Figure 11. Spectral Stokes parameters (I, Q and U) as well as the degree and angle of linear polarization as seen just above the water surface for microplastics of micrometric size (lognormal distribution centered on 1µm). Note that the remote sensing reflectance can be obtained by dividing *I* by π.

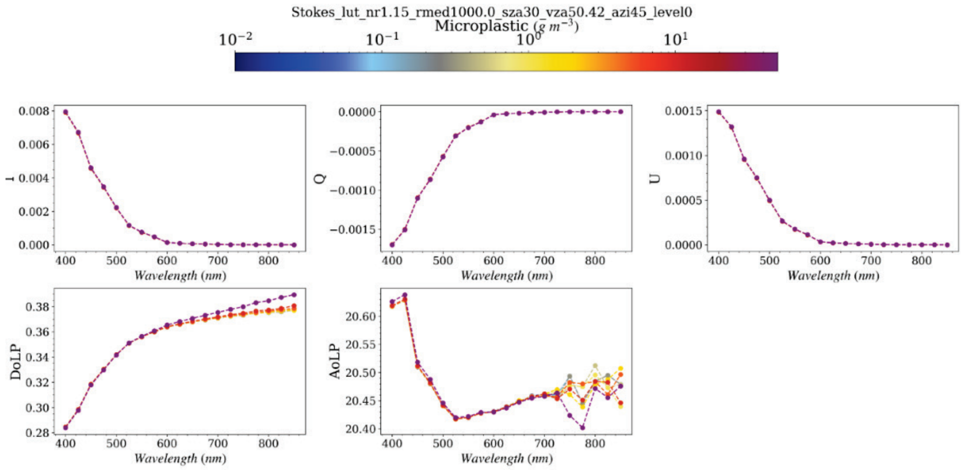

Figure 12. Similar to Figure 11 for microplastic size distribution centered on 1 mm. It can be readily observed that the signal is virtually insensible to the particle concentration for this millimetric size and assessed concentrations.

4.2 Synthetic satellite signal from in-situ data

Numerical simulations of the top-of-atmosphere (TOA) signal and specific satellite band response (called synthetic satellite data) were derived from actual reflectance measurements from the laboratory (Garaba et al., 2020; Knaeps et al., 2020; Moshtaghi et al., 2021). A first step was been to implement radiative transfer codes to input reflectance measurements of floating and submerged plastics followed by calculations to get hyperspectral TOA reflectance in presence of typical atmosphere and the reflectances obtained for several types of submerged plastics for different submersion depth and water clarity conditions (**Figure 13**).

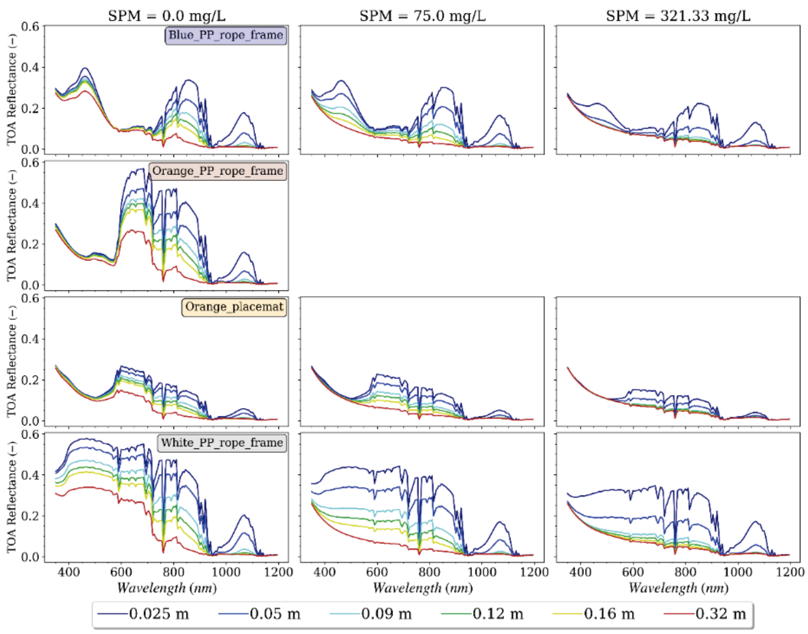

Figure 13. Top-of-atmosphere reflectance for the different configurations (depth/turbidity) obtained from laboratory measurements and radiative transfer propagation.

In order to quantify the information content of satellite measurements, we simulated the loss of information due to imperfect atmospheric correction e.g., uncertainties on aerosols parameters in state-of-the-art atmospheric correction algorithms. From those simulations, an ongoing work is dedicated to compute the response of the actual spectral bands of the major optical satellite missions (e.g., Sentinel-3, Sentinel-2, WorldView-3). The detailed findings of these simulations are reported in open-access (Garaba and Harmel, 2022).

5. Conclusion and outlook

Within the scope of the groundwork proposed, we established a reference data set consisting of a large and diverse sample of plastics, wave conditions, and lighting conditions, providing many opportunities for future scientific investigation. The limitations of the dataset are also discussed in terms of potential qualitative and quantitative analyses that can be performed thus also providing some hint on the research gaps.

The FLIR images will be used to determine the added value of polarization in the detection of individual macroplastics, which is currently often done using unpolarised RGB cameras, which face the challenge to consistently detect dark and translucent items. Because of its wide field-of-view and multiple spectral bands, as well as the different setups used in the experiment, the images are representative of multiple use cases including shipborne and UAV-based observations. The GroundSPEX spectra will be used to characterise the full linear spectro-polarimetric response of floating, submerged, and dry plastics. Such a data set can serve as the basis for NASA PACE-based marine plastic research. It is expected that the combined GroundSPEX-FLIR data set will be used for a more detailed analysis of the spectro-polarimetric response of marine plastics.

The data processing pipelines for the FLIR camera and GroundSPEX are still in development and the Python code is provided as open-source. A major opportunity to improve the FLIR camera data quality is to further investigate the demosaicking algorithm used to reconstruct RGB DOLP and AOLP from the RAW images. Different interpolation-based (Gao and Gruev, 2011) and Fourier transformation-based methods (Tyo et al., 2009) may provide significant improvements in the data quality and reductions of edge effects.

For future experiments with the FLIR camera, we recommend controlling the illumination on the target area, for instance by fully shading it except for a single light source. Reference RGB images are recommended for the GroundSPEX observations as supporting metadata.

An important limitation of the GroundSPEX data is the relative lack of angular diversity. While the instrument was used at two angles representative of the wider literature (40° and 57° from nadir), a much more diverse set of angles is necessary to fully characterize the Bidirectional Polarization Distribution Function (BPDF) of targets. The same is true for the halogen lamp next to GroundSPEX, which was aligned at arbitrary angles to provide maximum illumination. Future experiments with the goniometric setup to provide data with a wider range of illumination and observation angles.

GroundSPEX has a small field-of-view (<1° diameter) and was placed very close (<2 m) to the water surface in these experiments. This means that, in practice, the fill factor of plastics in its field-of-view was nearly always either 0% or 100%. Since most of the accumulations have likely fill factors of <10% in terms of plastic content, the polarization signatures detected with GroundSPEX will need to be converted to lower concentrations.

One of the project aims was to assess the satellite retrieval (plastic litter) algorithms for prospective application to the historic and next-generation polarimetric missions. During the course of the project it was challenging to obtain any satellite imagery but recently PARASOL data at 6 km pixel resolution was obtained and ongoing efforts will explore the polarimetric properties of known targets especially the Almeria greenhouse in Spain.

Through the activities of the non-governmental organisation “Expedition 7th Continent”, a data set of microplastics concentrations was gathered based on plankton net sampling in the North Atlantic gyre (Poulain et al., 2019). We used those concentrations to simulate the remote sensing signal for very oligotrophic water conditions representative of the North Atlantic gyre. Even if the observed sensitivity to plastics might appear small in comparison to more polluted areas, this can produce spurious interpretation of the satellite measurements in the oligotrophic gyres which are observed to track the sensitivity of the global ocean to climate change (Leonelli et al., 2022). To our knowledge, none of the research using remote sensing for such studies considered the potential alteration of the signal by microplastics to estimate the Chlorophyll-a concentration. This is one of the crucial outlooks of plastic-related remote sensing activities. In order to further our understanding on those interactions, the effort will have to be rooted to analysis of actual data both concerning the physicochemical properties and the radiometric implications. This is the goal of a dedicated oceanographic mission led by the NGO Expedition 7th Continent with the scientific support of T. Harmel. This mission is expected to gather new insights on the optical signal of nano- and microplastic and provide a validation data set for satellite applications.

6. References

Burggraaff, O., Schmidt, N., Zamorano, J., Pauly, K., Pascual, S., Tapia, C., Spyrakos, E., and Snik, F. (2019) Standardized spectral and radiometric calibration of consumer cameras. Optics Express, v. 27, no. 14, p. 19075-19101, doi:10.1364/OE.27.019075.

Gao, S., and Gruev, V. (2011) Bilinear and bicubic interpolation methods for division of focal plane polarimeters. Optics Express, v. 19, no. 27, p. 26161-26173, doi:10.1364/OE.19.026161.

Garaba, S. P., de Vries, R., Knaeps, E., Mijnendonckx, J., and Sterckx, S. (2020) Spectral reflectance measurements of dry and wet virgin plastics at varying water depth and water clarity from UV to SWIR (SEV-1). 4TU.Centre for Research Data, https://doi.org/10.4121/uuid:9ee3be54-9132-415a-aaf2-c7fbf32d2199.

Garaba, S. P., and Harmel, T. (2022) Top-of-atmosphere hyper and multispectral signatures of submerged plastic litter with changing water clarity and depth. Optics Express, v. 30, no. 10, p. 16553-16571, doi:10.1364/OE.451415.

Gilerson, A., Carrizo, C., Ibrahim, A., Foster, R., Harmel, T., El-Habashi, A., Lee, Z., Yu, X., Ladner, S., and Ondrusek, M. (2020) Hyperspectral polarimetric imaging of the water surface and retrieval of water optical parameters from multi-angular polarimetric data. Applied Optics, v. 59, no. 10, p. C8-C20, 10.1364/AO.59.0000C8.

Harmel, T., and Chami, M. (2013) Estimation of the sunglint radiance field from optical satellite imagery over open ocean: Multidirectional approach and polarization aspects. Journal of Geophysical Research: Oceans, v. 118, no. 1, p. 76-90, doi:10.1029/2012jc008221.

Hasekamp, O. P., Fu, G., Rusli, S. P., Wu, L., Di Noia, A., Brugh, J. a. d., Landgraf, J., Martijn Smit, J., Rietjens, J., and van Amerongen, A. (2019) Aerosol measurements by SPEXone on the NASA PACE mission: expected retrieval capabilities. Journal of Quantitative Spectroscopy and Radiative Transfer, v. 227, p. 170-184, doi:10.1016/j.jqsrt.2019.02.006.

Knaeps, E., Strackx, G., Meire, D., Sterckx, S., Mijnendonckx, J., and Moshtaghi, M. (2020) Hyperspectral reflectance of marine plastics in the VIS to SWIR. 4TU.Centre for Research Data, https://doi.org/10.4121/12896312.v2.

Leonelli, F. E., Bellacicco, M., Pitarch, J., Organelli, E., Buongiorno Nardelli, B., de Toma, V., Cammarota, C., Marullo, S., and Santoleri, R. (2022) Ultra-oligotrophic waters expansion in the North Atlantic Subtropical Gyre revealed by 21 years of satellite observations. Geophysical Research Letters, v. 49, no. 21, p. e2021GL096965, doi:10.1029/2021GL096965.

Mobley, C. D. (1999) Estimation of the remote-sensing reflectance from above-surface measurements. Applied Optics, v. 38, no. 36, p. 7442-7455, doi:10.1364/AO.38.007442.

Moshtaghi, M., Knaeps, E., Sterckx, S., Garaba, S., and Meire, D. (2021) Spectral reflectance of marine macroplastics in the VNIR and SWIR measured in a controlled environment. Scientific Reports, v. 11, no. 1, p. 5436, doi:10.1038/s41598-021-84867-6.

Poulain, M., Mercier, M. J., Brach, L., Martignac, M., Routaboul, C., Perez, E., Desjean, M. C., and ter Halle, A. (2019) Small microplastics as a main contributor to plastic mass balance in the North Atlantic subtropical gyre. Environmental Science & Technology, v. 53, no. 3, p. 1157-1164, doi:10.1021/acs.est.8b05458.

Tyo, J. S., LaCasse, C. F., and Ratliff, B. M. (2009) Total elimination of sampling errors in polarization imagery obtained with integrated microgrid polarimeters. Optics Letters, v. 34, no. 20, p. 3187-3189, doi:10.1364/OL.34.003187.

van Harten, G., de Boer, J., Rietjens, J. H. H., Di Noia, A., Snik, F., Volten, H., Smit, J. M., Hasekamp, O. P., Henzing, J. S., and Keller, C. U. (2014) Atmospheric aerosol characterization with a ground-based SPEX spectropolarimetric instrument. Atmospheric Measurement Techniques, v. 7, no. 12, p. 4341-4351, doi:10.5194/amt-7-4341-2014.